Kinematic Waves in the Isothermal Melt Spinning of Newtonian Fluids

Byung Min Kim and Jae Chun Hyun
Dept. of Chemical Engineering, Korea University, Seoul 136-701, Korea

Joo Seok Oh and Seung Jong Lee
Dept. of Chemical Engineering, Seoul National University, Seoul 151-742, Korea

The hyperbolic nature of the continuity equation in the melt spinning process causes several kinematic waves to travel in the spinline. Since different traveling waves possess different speeds, the system invariably has many characteristic times. This study computes the traveling times of these waves, finds their interrelationships, and then derives the criterion for the instability of periodic oscillation known as draw resonance. The period of oscillation is greater than the fluid residence time, but equal to the time during which both the maximum and minimum spinline cross-sectional area waves travel in sequence from the spinneret to the take-up. The onset of draw resonance occurs when two successive unity-throughput waves are also able to travel the same distance within the same period of oscillation. This happens when the drawdown ratio takes on the critical value of 20.218 for the isothermal spinning of Newtonian fluids, agreeing with the value reported by earlier researchers.

Introduction

The draw resonance that occurs in spinning processes, one of the major instabilities in polymer processing (see the comprehensive review by Petrie and Denn, 1976), arises as the drawdown ratio is increased beyond the known critical values and is manifested by a sustained periodic variation in the liquid cross-sectional area along the spinline. Since Christensen (1962) and Miller (1963) first discovered the phenomenon and named it as such, many research groups have conducted experimental/theoretical studies on this subject (Kase and Matsuo, 1965; Pearson and Matovich, 1969; Gelder, 1971; Donnelly and Weinberger, 1975; Ishihara and Kase, 1975; Fisher and Denn, 1976; Hyun, 1978; Blyer and Gieniewski, 1980; etc.). Thanks to these efforts, important aspects of the draw resonance have been brought out: (1) it is a hydrodynamic instability that does not need to be caused by fluid viscoelasticity, and so even viscous Newtonian fluids can exhibit it, and (2) the critical values of the drawdown ratio at the onset of draw resonance can be numerically computed if the governing equations with appropriate boundary conditions are given.

Correspondence concerning this article should be addressed to J. C. Hyun.
Present address of J. S. Oh: Research and Engineering Center, Han Hwa Group, Taejon 305-345, Korea.

In an attempt to further our understanding of the governing physics of the draw resonance, we focus in this study on the kinematic waves traveling in the spinline, and seek out the interrelationships among the traveling times of the different kinematic waves, to derive the criterion for the draw resonance.

Governing Equations and Numerical Simulation of the System

We treat the simple case of the isothermal melt spinning of Newtonian fluids, since more realistic cases have the same dynamic characteristics and the same criterion for instability. The governing equations of the system are the same as those used by other researchers (Kase and Matsuo, 1965; Gelder, 1971; Ishihara and Kase, 1975; Hyun and Ballman, 1978; Mewis and Petrie, 1987; etc.). The assumptions incorporated are as usual. First, all the secondary forces acting on the spinline, that is, inertia, gravity, surface tension, and air drag, are neglected to keep the rheological force only. (This assumption is a reasonable one unless the spinning velocity is very high and/or the spinning distance is extremely long.) Second, the velocity is uniform across a cross section of the spinline, and thus we have for the system a one-dimensional model involving the spinning distance coordinate only. Third, the origin of this distance coordinate is chosen where the extrudate swell occurs. (This assumption implies that our model includes neither the flow history prior to the spinneret nor the subsequent extrudate swell.)

Then the continuity equation is

$$\left[\frac{\partial A}{\partial t}\right]_x + \left[\frac{\partial (AV)}{\partial x}\right]_t = 0 \tag{1}$$

and the equation of motion is

$$\frac{\partial}{\partial x}\left[\eta_E A\left[\frac{\partial V}{\partial x}\right]_t\right]_t = 0. \tag{2}$$

The explanation for the variables appearing here are given in the Notation section.

The appropriate dimensionless initial and boundary conditions for the transient simulation of the system are

$$t=0:\quad A=A_s=A_0 r^{-x}=r^{-x},\quad V=V_s=V_0 r^x=r^x \quad \text{for} \quad 0<x<1 \tag{3}$$

$$t>0:\quad A=A_0=1, \quad \text{and} \quad V=V_0=1 \quad \text{at} \quad x=0 \tag{4}$$

$$V=V_L=V_0 r(1+\epsilon) \quad \text{at} \quad x=1, \tag{5}$$

where the subscripts S, 0, and L denote the steady-state solution, spinneret conditions, and take-up conditions, respectively, and ϵ is a constant representing the initial disturbance at the take-up to yield transient solutions.

The results of the numerical simulation with $r=20.218$ are shown in Figure 1 in the x-t grid of $2{,}000 \times 10{,}000$ mesh points guaranteeing acceptable accuracy. The transient curves (with the y axis representing the amplitudes of the oscillating spinline variables) with sufficient time elapsed after an initial disturbance of $\epsilon = 1\%$ at the take-up are those of the spinline cross-sectional area (A), velocity (V), throughput (AV), and tension (F) at five different spatial positions of the spinline: node 1, node 500 (¼-position of the whole spinning distance), node 1,000 (½-position), node 1,500 (¾-position), and node 2,000 (take-up position). The reason for picking out node 1 instead of the spinneret ($x=0$) is obvious: A, V, and AV are constant at the spinneret, as illustrated by Eq. 4, whereas they oscillate with time at all nodes. (The spinline tension F, on the other hand, oscillates with time at all positions, including the spinneret.)

We now make the following important observations from Figure 1. (1) All the curves are almost symmetrical in time, for we are very close to the onset point of instability, that is, r taking on its critical value (r_c) signaling the onset of draw resonance. (The curves are not symmetrical when $r<r_c$ because they decay with time, and they become highly skewed as r gets larger than r_c, as shown in Figure 2.) (2) The spinline tension (F) curve is the same at all nodes, that is, independent of x, which is the direct result of the equation of motion, Eq. 2, based on the assumption of the negligible sec-

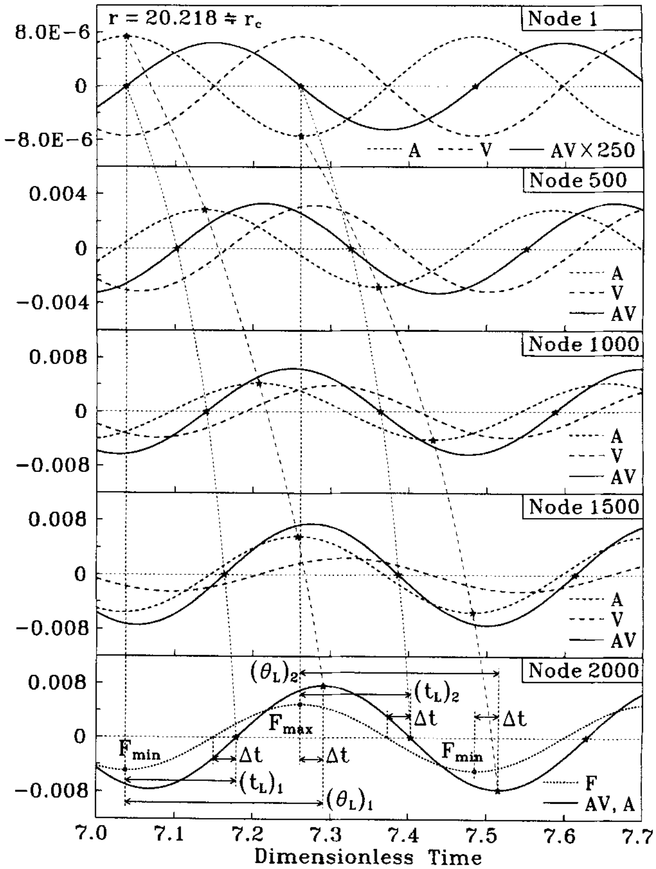

Figure 1. Transient curves of spinline variables at five different spatial positions of the spinline when $r = 20.218 \doteqdot r_c$.

ondary forces. (3) This F turns out to precede the cross-sectional area (A) wave at the take-up by Δt in time. This is because from Eq. 2 we have

$$\eta_E A[\partial V/\partial x]_t = F(t), \tag{6}$$

where we can readily see that A and F cannot be in phase unless $[\partial V/\partial x]_t$ is too. Moreover from the fact that the attenuation of A is caused by the force F, we can see that F should lead A. (4) When the spinline tension F is maximum (F_{max}) in time, velocity is maximum (V_{max}), at node 1, and the cross-sectional area minimum (A_{min}). This is a very important point as explained below. When the maximum tension acts on the spinline, it increases the velocity and reduces the cross-sectional area everywhere on the spinline as compared to the moment when the steady-state force acts. The impact of this maximum force is highest at node 1, because it is impossible to transfer this force effect to the next node up in the spinline, because at the next position, the spinneret, V and A are always held constant. Therefore, at node 1 V and A become maximum and minimum respectively, with time. The simulation results indeed reveal that at node 1 V_{max} and A_{min} occur at the moment of F_{max}. When F is at its minimum (F_{min}) on the spinline, the opposite situation prevails, that is, V_{min} and A_{max} occur at node 1. (5) There are several waves traveling along the spinline: A, constant-A, constant-V,

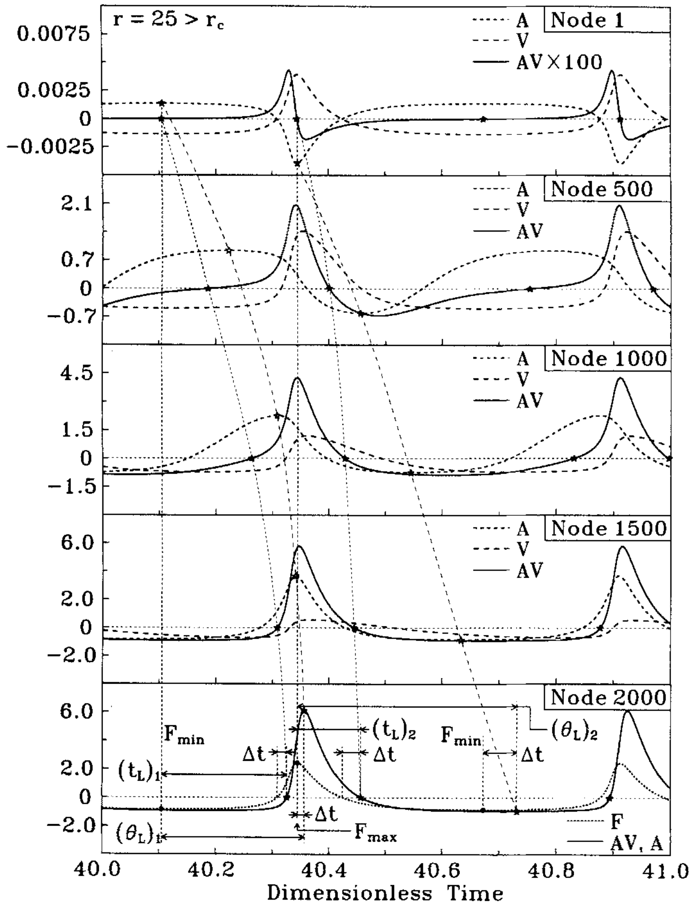

Figure 2. Transient curves of the spinline variables at five different spatial positions of the spinline when $r = 25 > r_c$.

constant-AV, and A_{max} and A_{min}. Except for the A waves, which are the same as the fluid elements and thus travel with the spinline velocity V, the other types of waves have their own unique traveling speeds, which are different from V. We will elaborate on this point in the next section. (6) Among the waves just listed, the most important ones for our study are A_{max} and A_{min}, and constant-AV waves, as explained later. From Figure 1, we can see that when $r = 20.218$, A_{max} (or A_{min}) waves starting from node 1 at the moment of F_{min} (or F_{max}), arrive at the take-up in the time of $(T/2 + \Delta t)$, whereas unity-AV ($AV = 1$) waves starting from node 1 at the moment of F_{min} (or F_{max}) arrive at the take-up in the time of $(T/4 + \Delta t)$. Here T is the period of the oscillation and Δt is the time (phase) differences between the F curve and A curve at the take-up.

Kinematic Waves Equations and their Traveling Speeds

Now we study the six different waves mentioned earlier, in terms of their governing equations and traveling speeds. First, consider A waves. As explained before, these are the same as the fluid element waves, since from Eq. 1 we get

$$\left[\frac{\partial A}{\partial t}\right]_x + V\left[\frac{\partial A}{\partial x}\right]_t = -A\left[\frac{\partial V}{\partial x}\right]_t \tag{7}$$

which tells us that A waves travel with speed V, and their magnitudes decrease as they go down the spinline because the righthand side of Eq. 7 is always negative, being equal to $-F(t)/\eta_E$, as shown in Eq. 6. Since the velocity V denotes the speed of fluid elements, here we can write

$$V \equiv [\partial x/\partial t]_{f.e.} \tag{8}$$

Second, the governing equation of constant-A waves is derived from Eq. 1 as follows:

$$\left[\frac{\partial A}{\partial t}\right]_x + Y_1\left[\frac{\partial A}{\partial x}\right]_t = 0, \tag{9}$$

where

$$Y_1 \equiv \left[\frac{\partial x}{\partial t}\right]_A = -\frac{\left[\frac{\partial A}{\partial t}\right]_x}{\left[\frac{\partial A}{\partial x}\right]_t}$$

$$= \frac{\left[\frac{\partial (AV)}{\partial x}\right]_t}{\left[\frac{\partial A}{\partial x}\right]_t} = \left[\frac{\partial (AV)}{\partial A}\right]_t = V + A\left[\frac{\partial V}{\partial A}\right]_t. \tag{10}$$

Equation 9 shows that these constant-A waves don't change their magnitudes as they travel in the spinline with the speed Y_1, whose values can be numerically computed using Eq. 10. Third, the governing equation of constant-V waves can also be derived similarly:

$$\left[\frac{\partial V}{\partial t}\right]_x + Y_2\left[\frac{\partial V}{\partial x}\right]_t = 0, \tag{11}$$

where

$$Y_2 \equiv \left[\frac{\partial x}{\partial t}\right]_V = -\frac{\left[\frac{\partial V}{\partial t}\right]_x}{\left[\frac{\partial V}{\partial x}\right]_t}. \tag{12}$$

Unlike Y_1 in Eq. 10, the expression for the speed Y_2 of the constant-V waves is not simplified further, for Eq. 1 cannot be utilized in Eq. 12. Fourth, the governing equation of the constant-throughput (AV) waves is derived from Eq. 1 in the same manner as that of the constant-A waves shown in Eqs. 9 and 10:

$$\left[\frac{\partial (AV)}{\partial t}\right]_x + U\left[\frac{\partial (AV)}{\partial x}\right]_t = 0, \tag{13}$$

where

$$U \equiv \left[\frac{\partial x}{\partial t}\right]_{AV} = -\frac{\left[\frac{\partial(AV)}{\partial t}\right]_x}{\left[\frac{\partial(AV)}{\partial x}\right]_t} = \frac{\left[\frac{\partial(AV)}{\partial t}\right]_x}{\left[\frac{\partial A}{\partial t}\right]_x}$$

$$= \left[\frac{\partial(AV)}{\partial A}\right]_x = V + A\left[\frac{\partial V}{\partial A}\right]_x. \quad (14)$$

Again, Eq. 13 tells us that the throughput waves don't change their magnitude as they travel in the spinline with speed U, whose values can be numerically computed using Eq. 14.

Finally, we consider the A_{max} and A_{min} waves, which satisfy the condition of $[\partial A/\partial t]_x = 0$. Unlike the four kinds of waves illustrated earlier, these waves don't yield any convenient expressions for their traveling speeds. We nonetheless adopt similar notations here as before:

$$W \equiv [\partial x/\partial t]_{A\,max} \quad \text{or} \quad [\partial x/\partial t]_{A\,min}. \quad (15)$$

It is these A_{max} and A_{min} waves that directly determine the period of the oscillation of the system, as shown in Figure 1. The mechanism of the oscillation played by these A_{max} and A_{min} waves is explained as follows. After an A_{max} wave appears at node 1 at the moment of the minimum spinline tension, F_{min}, it travels down the spinline and goes through the take-up. As this A_{max} wave passes through the take-up, the spinline tension becomes maximum because the tension is proportional to the area as in Eq. 6. This maximum tension occurs, though, Δt before the moment of A_{max} arrives at the take-up. This difference, Δt, is the result of the fact that F leads A, as explained in Eq. 6. This maximum tension acting on the entire spinline, in turn, causes a minimum A wave, A_{min}, to appear at node 1 and to travel toward the take-up. As this A_{min} wave passes through the take-up, the spinline tension becomes minimum, F_{min}, occurring Δt before the moment A_{min} arrives at the take-up. Then this minimum force, F_{min}, causes a maximum area, A_{max}, to appear at node 1, and the cycle repeats itself.

We have just explained how the oscillation persists as A_{max} and A_{min} waves caused by F_{min} and F_{max}, respectively, continually appear at node 1 in sequence. The period of the oscillation is thus expressed as follows.

$$T = [(\text{traveling time of an } A_{max} \text{ wave}) - \Delta t]_1 + [(\text{traveling time of an } A_{min} \text{ wave}) - \Delta t]_2 \equiv [\theta_L - \Delta t]_1 + [\theta_L - \Delta t]_2, \quad (16)$$

where

$$\theta_L = \int_{x_1}^{1} \frac{dx}{W}, \quad (17)$$

and x_1 represents node 1, W is given by Eq. 15, and the subscripts 1 and 2 denote the respective waves starting at the moments of F_{min} and F_{max}.

Criterion for Draw Resonance

Only two kinematic waves travel the entire distance from the spinneret to the take-up: A (fluid element) waves and unity-throughput ($AV = 1$) waves. The ones traveling from node 1 to the take-up are the A_{max} and A_{min} waves. The constant-A, constant-V, and nonunity-throughput waves travel only part of the spinning distance. Here is why. Since the value of throughput is always unity at the spinneret, among infinitely many throughput waves, only unity-throughput waves travel the entire spinning distance. Second, A or V of the constant-A or constant-V waves, respectively, cannot stay at constant values for the entire spinning distance, because the spinline has to be attenuated (i.e., A is reduced) and accelerated (i.e., V is increased) at the take-up compared with at the spinneret, as Eqs. 4 and 5 require.

As in Eq. 17, the travel times of two more kinematic waves are defined as follows:

$$\tau_L = \int_0^1 \frac{dx}{V}, \qquad t_L = \int_0^1 \frac{dx}{U_{AV=1.0}}. \quad (18)$$

Thus τ_L denotes the travel time of the A waves, that is, the fluid residence time, and t_L denotes the travel time of the unity-throughput ($AV = 1$) waves.

As mentioned before, the unity-throughput waves travel the entire spinning distance in the time $(T/4 + \Delta t)$ when r is at its critical value r_c. It turns out, however, that when r is smaller than r_c, that is, the system being stable, t_L is larger than $(T/4 + \Delta t)$. In other words, we have the following relation for $r \le r_c$:

$$(t_L - \Delta t)_1 + T/4 + (t_L - \Delta t)_2 + T/4 \ge [\theta_L - \Delta t]_1 + [\theta_L - \Delta t]_2 = T$$

or

$$(t_L)_1 + (t_L)_2 + T/2 \ge (\theta_L)_1 + (\theta_L)_2, \quad (19)$$

where the equality represents the onset of draw resonance at $r = r_c$.

Relation 19 thus becomes the criterion for draw resonance. This can be explained as follows. While the period of the oscillation T is determined by the travel times of A_{max} and A_{min} together with Δt as shown in Eq. 16, in order for the oscillation to be sustained, the two successive unity-throughput waves also need to fit into the picture, that is, need to be able to travel the same distance within the same period. This is because, as explained before, they are also the waves to travel the entire spinning distance. However, for $r < r_c$, the required time for these two successive unity-throughput waves to travel (the lefthand side of Eq. 19) becomes larger than the available time (the righthand side of Eq. 19), which thus makes the oscillations impossible, that is, the oscillations die out with time. At $r = r_c$, the two times in Eq. 19 become equal, and thus the equality holds, and also the travel times of the waves with subscripts 1 and 2 become *identical* to each other. As r is increased beyond r_c, the inequality of Eq. 19 becomes reversed, that is, the required time gets smaller than the allowed time. Thus the sustained oscillation is always

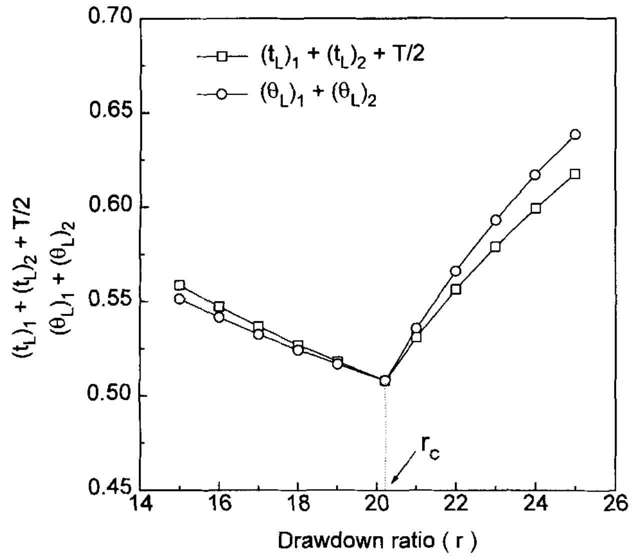

Figure 3. Required traveling time for two successive unity-throughput waves, and allowed traveling time by A_{max} and A_{min} waves plotted against drawdown ratio, *r*.

possible, with the transient curves becoming highly skewed and having large amplitudes as shown in Figure 2. Figure 3 shows how both the left and right sides of Eq. 19 change with r.

In order to clearly demonstrate the traveling kinematic waves, we include one more graph here. Figure 4 shows the picture, when $r = 20.218$, of the characteristics of the differential equation, Eq. 13, in the x-t plane, which are also the contours of constant-AV waves. Here, we see not only the trajectories of the unity-throughput waves with their travel times, $t_L = 0.1419$, but we also can see the trajectories of the A_{max} and A_{min} waves with their travel times $\theta_L = 0.2538$. ($T = 0.4484$, $\tau_L = 0.3162$, $\Delta t = 0.0298$.) This is because the A_{max} and A_{min} waves follow, by definition, the loci of $[\partial A/\partial t]_x = 0$, which in turn are identical to the loci of $[\partial(AV)/\partial x]_t = 0$ due to Eq. 1. These loci are easy to track down, as shown in Figure 4.

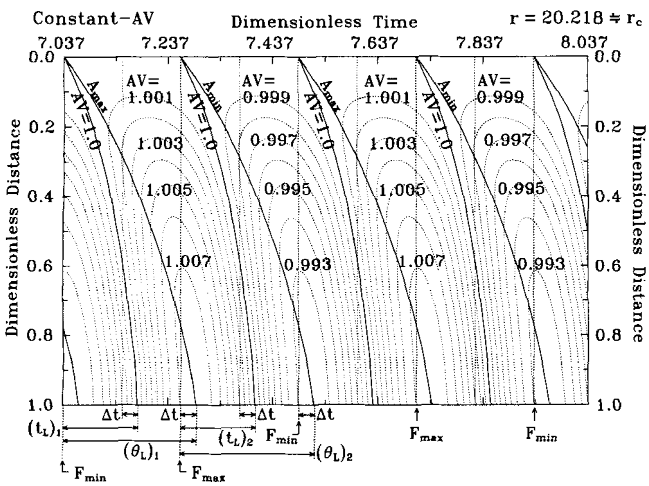

Figure 4. Characteristics (contours of constant-*AV* waves) when *r* = 20.218.

We also note here that the period (T) of the oscillation is larger than the fluid residence time (τ_L).

Conclusion

The spinline oscillation in melt spinning is caused by the continuity equation, which is a hyperbolic differential equation making many kinematic waves travel along the spinline. The period of this oscillation has been found to be larger than the fluid residence time but equal to the time during which both the maximum and minimum spinline cross-sectional area waves in sequence travel from the spinneret to the take-up. The criterion for draw resonance is provided by the comparison of the two characteristic times of the system, that is, the required time for the two successive unity-throughput waves to travel the spinning distance vs. the available time provided by the traveling times of the A_{max} and A_{min} waves. Depending on whether the drawdown ratio is smaller than, equal to, or larger than the critical value, the required time becomes larger than, equal to, or smaller than the available time, respectively, which makes the sustained oscillations of draw resonance impossible, just possible, or always possible, respectively.

Acknowledgments

The work was supported by the Korean Science and Engineering Foundation under Grant 93-0300-02-01-3. We would like to thank Prof. M. M. Denn, University of California, Berkeley, for his original questions pointing out errors in the earlier paper by one of the present authors.

Notation

- A = dimensionless spinline cross-sectional area = spinline cross-sectional area divided by that at the spinneret
- F = dimensionless spinline tension force
- L = spinning distance from the spinneret to the take-up
- r = drawdown ratio
- r_c = critical drawdown ratio at the onset of draw resonance
- T = dimensionless period of draw resonance
- t = dimensionless time = time multiplied by the spinline velocity at the spinneret and divided by the distance from the spinneret to the take-up
- t_L = dimensionless traveling time of unity-throughput waves from the spinneret to the take-up
- U = dimensionless traveling speed of throughput waves
- V = dimensionless spinline velocity = spinline velocity divided by the spinline velocity at the spinneret
- W = dimensionless traveling speed of A_{max} or A_{min} waves
- x = dimensionless distance from the spinneret = distance from the spinneret divided by the distance from the spinneret to the take-up
- Y_1 = dimensionless traveling speed of constant-A waves
- Y_2 = dimensionless traveling speed of constant-V waves
- Δt = dimensionless time (phase) differences between the F curve and A curve at the take-up
- η_E = dimensionless spinline extensional viscosity = spinline extensional viscosity divided by the spinline extensional viscosity at the spinneret
- θ_L = dimensionless traveling time of A_{max} or A_{min} waves from node 1 to the take-up
- τ_L = dimensionless traveling time of spinline cross-sectional area (fluid elements) waves from the spinneret to the take-up

Literature Cited

Blyler, L. L., and C. Gieniewski, "Melt Spinning and Draw Resonance Studies on a Poly(α-methyl Styrene/Silicone) Block Copolymer," *Poly. Eng. Sci.*, **20**, 140 (1980).

Christensen, R. E., "Extrusion Coating of Polypropylene," *SPE J.*, **18**, 751 (1962).
Donnelly, G. J., and C. B. Weinberger, "Stability of Isothermal Fiber Spinning of a Newtonian Fluid," *Ind. Eng. Chem. Fundam.*, **14**, 334 (1975).
Fisher, R. J., and M. M. Denn, "A Theory of Isothermal Melt Spinning and Draw Resonance," *AIChE J.*, **22**, 236 (1976).
Gelder, D., "The Stability of Fiber Drawing Processes," *Ind. Eng. Chem. Fundam.*, **10**, 534 (1971).
Hyun, J. C., "Theory of Draw Resonance: I. Newtonian Fluids," *AIChE J.*, **24**, 418 (1978); also "Part II. Power-law and Maxwell Fluids," **24**, 423 (1978).
Hyun, J. C., and R. L. Ballman, "Isothermal Melt Spinning—Lagrangian and Eulerian Viewpoints," *J. Rheol.*, **22**, 349 (1978).
Ishihara, H., and S. Kase, "Studies on Melt Spinning. V. Draw Resonance as a Limit Cycle," *J. Appl. Poly. Sci.*, **19**, 557 (1975).
Kase, S., and T. Matsuo, "Studies on Melt Spinning. I. Fundamental Equations on the Dynamics of Melt Spinning," *J. Poly. Sci., Part A*, **3**, 2541 (1965).
Mewis, J., and C. J. S. Petrie, "Hydrodynamics of Spinning Polymers," *Encyclopedia of Fluid Mechanics*, Gulf Publishing, Houston, Vol. 6, N. P. Cheremisinoff, ed., p. 111 (1987).
Miller, J. C., "Swelling Behavior of Extrusion," *SPE Trans.*, **3**, 134 (1963).
Pearson, J. R. A., and M. A. Matovich, "Spinning a Molten Threadline: Stability," *Ind. Eng. Chem. Fundam.*, **8**, 605 (1969).
Petrie, C. J. S., and M. M. Denn, "Instabilities in Polymer Processing," *AIChE J.*, **22**, 209 (1976).

Manuscript received Jan. 16, 1996, and revision received Apr. 29, 1996.